NONLINEAR OPTICAL PHENOMENA

PACS numbers: 42.81.Dp; 42.65.Ky
DOI: 10.1070/QE2005v035n08ABEH010357

Four-wave mixing in two-layer microstructure fibres

Yu.P. Yatsenko, A.E. Levchenko, A.D. Pryamikov, A.F. Kosolapov, S.L. Semenov, E.M. Dianov

***Abstract*. The dispersion and waveguide characteristics of two-layer microstructure fibres with different layer filling factors are studied theoretically and experimentally. It is shown that by changing the filling factor of the second layer, it is possible to achieve lower effective cross sections for a mode and to control dispersion characteristics in a broader range. Frequency conversion during four-wave mixing with a frequency shift of 5460 cm^{-1} (1098 – 687 nm) and efficiency of 0.1 % at 200 mW of cw pump power was obtained for the first time in two-layer fibres fabricated for experiments.**

Keywords: *microstructure fibres, dispersion, nonlinearity coefficient, four-wave mixing, parametric frequency conversion.*

1. Introduction

The efficient frequency conversion from the visible and IR ranges to telecommunication ranges at 1.3 and 1.5 μm by means of fibre frequency converters is an urgent and challenging problem. Such converters use, as a rule, four-wave mixing ($2\omega_p = \omega_a + \omega_s$) in which two pump photons ω_p create a pair of photons at the Stokes (ω_s) and anti-Stokes (ω_a) frequencies. For such a process to be efficient, fibres are required that, first, should have large nonlinearity coefficients $\gamma = 2\pi n_2/\lambda A_{eff}$ (where n_2 is the nonlinear refractive index, λ is the wavelength, and A_{eff} is the effective area of the mode) and, second, they should have dispersion characteristics allowing one to obtain sufficiently large coherence lengths $L_{coh} = \pi/\Delta k$ (Δk is the phase mismatch of wave vectors) at which the phase matching condition is fulfilled for interaction waves [1].

Currently great progress was achieved in the fabrication of germanosilicate fibres with a core heavily doped with GeO_2 [2] and also of TeO_2- [3] and Bi_2O_3-doped [4] fibres having large nonlinearity coefficients ($\gamma \sim 100 - 1000$ W^{-1} km^{-1}). However, the dispersion zero in usual step-index fibres is strongly shifted to the IR region ($\lambda_0 >$ 1.5 μm). For four-wave mixing in the wavelength range shorter than 1.5 μm, this means a large phase mismatch between wave vectors due to material dispersion.

The material dispersion can be compensated in principle by using the intermode dispersion in multimode fibres [5] and polarisation dispersion in polarisation-preserving single-mode fibres [6]. However, in the first case the conversion efficiency decreases due to a decrease in the overlap integrals caused by the involvement of higher-order modes in the process. In the second case, the four-wave mixing efficiency decreases due to a lower value of the nonlinear refractive index n_2 for orthogonal polarisations.

In the last years, a new direction in the fabrication technology of optical fibres is being extensively developed – the fabrication of microstructure fibres having several layers of holes filled with air symmetrically arranged around the core [7 – 9]. They possess unique dispersion properties, which, in particular, allow one to shift the dispersion zero of silica fibres to the blue ($\lambda_0 < 0.8$ μm) by preserving the single-mode regime in a very broad spectral range. These properties are very important for the development of the efficient fibre frequency converters in the range from 0.6 to 1.5 μm. Thus, for any frequency shift in this range, it is possible, by adjusting parameters (in particular, the layer filling factor $\kappa = d/\Lambda$, where d is the hole diameter and Λ is the distance between holes), to fit the dispersion zero to the pump wave required for this shift. In this case, it becomes possible to compensate the material dispersion by the waveguide dispersion even for large frequency shifts by preserving the single-mode propagation for all the interacting waves.

The first successful experiments on four-wave mixing in microstructure fibres with the blue-shifted dispersion zero were performed in papers [10, 11], where fibres manufactured by the capillary method were used, which had the hexagonal hole symmetry and many layers (more than six). The method for manufacturing such multilayer fibres is rather time-consuming.

In this paper, we studied for the first time the parametric frequency conversion in two-layer fibres fabricated by using the original method, which substantially simplifies the technological process. We showed that two-layer SiO_2 fibres with different filling parameters of the layers have the region of parameters where the waveguide losses and the effective region of the mode are sufficiently small, which allows the parametric frequency conversion with the shift exceeding 5000 cm^{-1} upon pumping by a cw Ti : sapphire laser.

Yu.P. Yatsenko, A.E. Levchenko, A.D. Pryamikov, A.F. Kosolapov, S.L. Semenov, E.M. Dianov Fiber Optics Research Center, A.M. Prokhorov General Physics Institute, Russian Academy of Sciences, ul. Vavilova 38, 119991 Moscow, Russia; e-mail: yuria@fo.gpi.ru, andrlevc@fo.gpi.ru

Received 14 June 2005
Kvantovaya Elektronika **35** (8) 715 – 719 (2005)
Translated by M.N. Sapozhnikov

2. Dispersion and waveguide characteristics of two-layer fibres. The numerical analysis

The value of the blue shift of the dispersion zero in microstructure fibres is directly related to the layer filling factor κ [12]. The larger κ, the larger blue shift of the dispersion curve can be obtained. The numerical analysis and experiments [13, 14] showed that the blue shift of the dispersion zero in fibres with a hexagonal structure of identical holes is accompanied by the decrease in the effective mode area and, hence, by the increase in the nonlinearity coefficient.

The increase in the filling factor has another positive aspect, which is important for technology: the number of layers required to obtain low waveguide losses decreases with increasing filling factor [15]. It follows from [15] that to obtain the waveguide losses lower than 10 dB km^{-1}, two-layer waveguides should have $\kappa > 0.8$. To perform frequency conversion in a given spectral range, the dispersion zero should have a certain position, which depends on the slope of the dispersion curve and frequency shift. In fibres with the same geometry of holes, such a dispersion characteristic may not correspond to the condition of the maximum possible filling factor and, hence, to the minimal effective mode area. It was shown in [16–18] that in the case of multilayer fibres the inhomogeneous distribution of holes in layers substantially affects dispersion characteristics.

We calculated numerically the waveguide characteristics of two-layer fibres with the different geometry of holes in layers. The calculation was performed by the method of finite elements by using the standard Femlab (version 7) program to solve the vector equation for mode fields in microstructure fibres.

Figure 1 shows the wavelength dependences of the dispersion D and the effective mode area A_{eff} for two-layer fibre A with identical layer filling factors ($\kappa_1 = \kappa_2 = 0.69$) and fibre B with $\kappa_1 = 0.69$ and $\kappa_2 = 0.96$. One can see that for these filling factors the differences between these fibres appear only for small A_{eff} ($\Lambda < 0.92$ μm). They are manifested in a broader wavelength region of the guided propagation of the fundamental mode and in a larger shift of dispersion zeroes upon changing the parameters of fibre B having 1.4 times larger κ_2. Thus, for $\Lambda = 0.69$ μm in fibre A, the wavelength region where the guided propagation of the HE_{11} mode is possible for effective mode area differing by no more than 1.5 times does not exceed 0.95 μm in the long-wavelength region. In fibre B, this region extends to 1.2 μm. The distance between the first and second dispersion zeroes in the dispersion curves increases in fibre B by a factor of 1.6 for $\Lambda = 0.92$ μm and 4.7 for $\Lambda = 0.69$ μm.

Stronger differences between the wavelength dependences of the dispersion and effective mode area for fibres with different filling factors are demonstrated in Fig. 2, where the results are presented for fibres C and D with $\kappa_1 = 0.4$ (which is 1.7 times lower than κ_1 for fibres A and B) and the values of κ_2 differing by a factor of 1.5. For fibre D with a greater value of κ_2, not only the wavelength range expands in which the effective mode area changes weakly, but also the mode field becomes more strongly localised, resulting in the decrease in A_{eff} by ~ 10 %. It is also important that the difference in κ_2 by a factor of 1.5 results in a strong difference between the dispersion characteristics of these fibres. The inset in Fig. 2 shows that the dispersion curve for fibre C has two dispersion zeroes in the 1-μm region, whereas the dispersion curve for fibre D has only one zero in the vicinity of which the slope of the dispersion characteristic is much smaller.

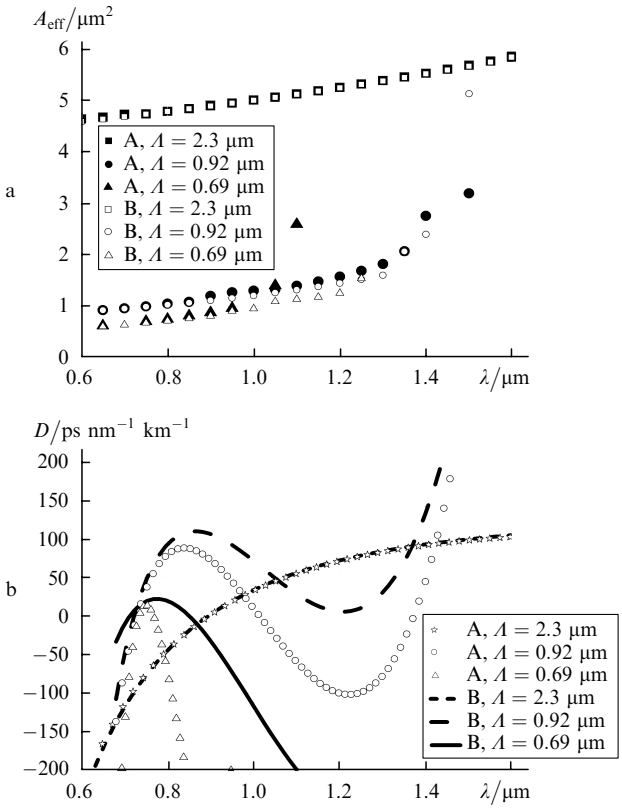

Figure 1. Dependences of the effective mode area (a) and dispersion (b) on the wavelength for two-layer fibre A with identical layer filling factors ($\kappa_1 = \kappa_2 = 0.69$) and two-layer fibre B with $\kappa_1 = 0.69$ and $\kappa_2 = 0.96$ for different Λ.

Therefore, our analysis shows that variation of the filling factor κ_2 of two-layer microstructure fibres allows one to minimise the effective mode area and to control the

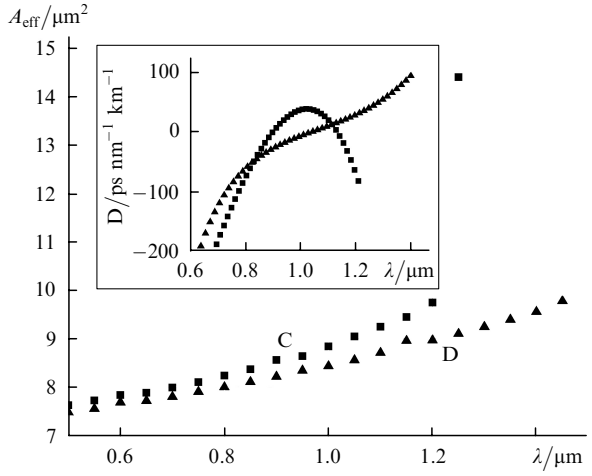

Figure 2. Dependences of the effective mode area and dispersion (insert) on the wavelength for two-layer fibre C with identical layer filling factors ($\Lambda = 2.3$ μm, $\kappa_1 = \kappa_2 = 0.4$) and fibre D with $\Lambda = 2.3$ μm, $\kappa_1 = 0.4$ and $\kappa_2 = 0.6$.

dispersion zero and the slope of the dispersion curve in a broader spectral range. This is especially important upon four-wave mixing frequency conversion from the visible to telecommunication range because this requires the presence of the dispersion zero in the 1-μm region and a small effective area of the mode. One can see from Figs 1 and 2 that this can be achieved by varying the factor κ_2.

3. Experimental

We fabricated two two-layer fibres with parameters presented in Table 1, where the parameters of a typical multilayer fibre (fibre No. 1) fabricated by the capillary method are also given. The latter fibre had holes of the same geometry and was used as a reference in experiments.

Table 1.

Fibre number	Number of layers	d_0/ μm	κ_1	κ_2	λ_0/ nm	A_{eff}/ μm^2	γ/ W^{-1} km^{-1}
1	4	6.2	0.52	0.52	1129	32	4
2	2	2.9	0.75	0.79	874	4.86	26
3	2	2.8	0.82	0.88	858	4.24	30

The preform from which fibres No. 2 and 3 were drawn was fabricated by mechanical drilling. An F-300 glass rod (Heraus) of diameter 22 mm and height 100 mm was mechanically drilled with a tube instrument with a diamond crown. Note that the fabrication of microstructure preforms by mechanical drilling offers a number of advantages compared to the capillary and extrusion methods. In particular, almost all kinds of glasses, except strongly strained, can be drilled. A complicated geometrical structure of holes can be simpler produced by using mechanical drilling, and in addition this method also substantially reduces the number of technological operations.

The drilled preform was etched, drawn, and jacketed (a silica tube was fused on the preform to increase its outer diameter). Thermal processing was performed in the flame of an oxygen-hydrogen burner. This resulted in the polishing of the internal surface of holes. During drawing and jacketing, a noble gas at an excess pressure was introduced into internal holes to compensate for surface tension forces tending to collapse the holes. By adjusting properly the pressure in holes and the temperature gradient in the preform, we managed to increase selectively the diameter of holes in the second layer. The preform manufactured in this way was drawn to a fibre. During drawing, pressure in holes was controlled and varied. By varying pressure in holes, we fabricated from one preform a series of fibres with the hexagonal symmetry and different geometries of holes.

The wavelength dependences of optical losses in fibres are presented in Fig. 3. The absorption bands at 0.95, 1.24, and 1.4 μm are related to the vibrational overtones of hydroxyl groups. The OH groups were introduced to the glass matrix from the burner flame during thermal processing. One can see from Fig. 3 that absorption losses outside the 1.4-μm band in two-layer fibres are lower than in multilayer fibre No. 1. The dispersion curves in Fig. 4 were obtained by the interference method [19, 20]. Two-layer fibres with a higher filling factor ($\kappa = 0.75 - 0.88$) compared to multilayer fibre No. 1 ($\kappa = 0.52$) have the dispersion zero shifted to the blue and a greater slope of the dispersion curves.

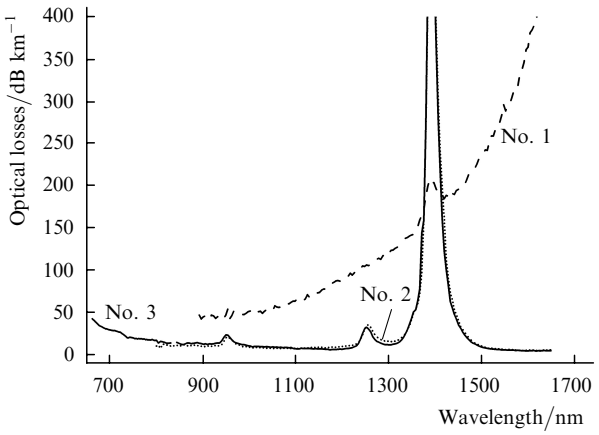

Figure 3. Waveguide losses measured for fibres presented in Table 1.

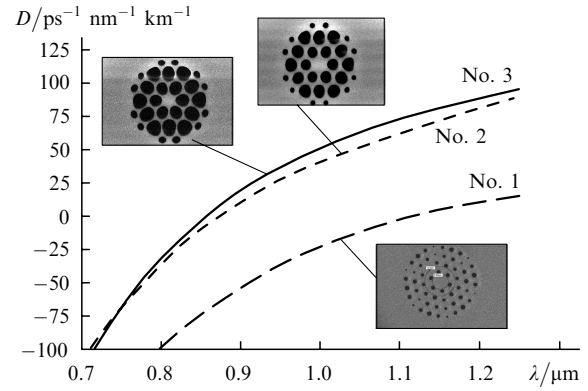

Figure 4. Dispersion curves measured for fibres No. 1–3. Inserts show the electron-microscope photographs of fibre ends.

Four-wave mixing experiments were performed on the setup schematically shown in Fig. 5. It consists of a 2-W cw Ti : sapphire laser with a 0.1-nm linewidth tunable in the range from 700 to 870 nm and a diode-pumped cw Yb-doped fibre laser emitting at 1098 nm. The tunable Ti : sapphire laser had a four-mirror Z-shaped resonator. A three-plate Lyot filter mounted in front of the output mirror was used as a selective element. The Yb-doped fibre laser consisted of a 100-mW master oscillator and a power

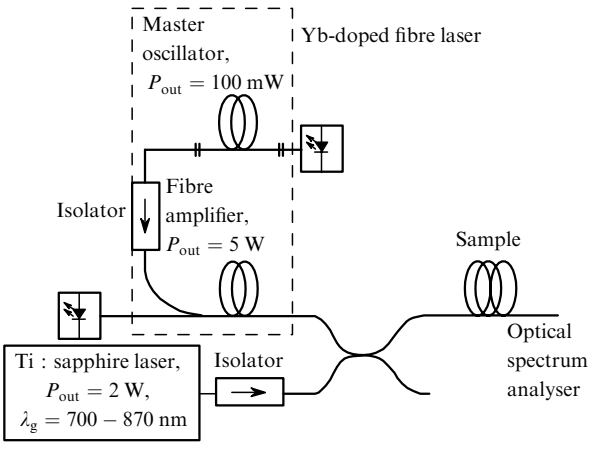

Figure 5. Scheme of the experimental setup.

amplifier providing the output power up to 5 W in the laser line of width 0.1 nm. Radiation from the Ti : sapphire and Yb-doped fibre lasers was coupled through a broadband coupler into a microstructure fibre. The effect of back-scattered radiation was excluded by means of optical isolators. The emission spectrum at the fibre output was recorded with an optical spectrum analyser.

4. Parametric frequency conversion. Results and discussion

The gain of a signal upon four-wave mixing frequency conversion is determined by the expression [1]

$$g = \left[(\gamma P_0)^2 - \left(\frac{\Delta k}{2}\right)^2\right]^{1/2}.$$

The phase mismatch $\Delta k = \Delta\beta_w + \Delta\beta_{nl}$ of the wave vectors is determined by the waveguide component β_w equal to the difference of propagation constants of the interacting waves $\Delta\beta_w = \beta_s + \beta_a - 2\beta_p$ (where β_s, β_a, and β_p are the propagation constants of the Stokes and anti-Stokes waves and the pump wave, respectively) and the nonlinear term $\Delta\beta_{nl} = 2\gamma P_0$ depending on the pump power P_0. It is known that the maximum gain in a single-mode fibre corresponding to the phase-matching condition $\Delta k = 0$ can be obtained only for the pump waves near the dispersion zero.

Figure 6 shows the Stokes and anti-Stokes shifts, for which the phase-matching condition is satisfied, calculated for fibres No. 1–3 as functions of the pump wavelength. The calculations were performed by expanding the propagation constant β in a Taylor series in the vicinity of the pump wavelength. All the higher even derivatives up to the eight order used in the phase-matching condition were calculated from the second-order dispersion curve measured for each fibre. As follows from the curves, the frequency shift for all fibres strongly depends on the pump-wavelength detuning from the zero dispersion wavelength. This fact was already pointed out by the authors of papers [10, 11] for the case of multilayer microstructure fibres. The growth of the frequency-shift curve correlates with the slope of the dispersion curve, and therefore it is higher for fibre No. 3 having the greatest filling factor.

We performed frequency conversion in all fibres of three types by using radiation from a 200-mW tunable cw Ti : sapphire laser and a 600-mW cw Yb-doped fibre laser. The experimental frequency shifts (Fig. 6 and Table 2) agree with the theoretical ones within 10 %. (Noticeably larger deviations for the Stokes region are related to the insufficient number of experimental points on the dispersion curves in the wavelength region above 1.3 μm.)

Fibre No. 1 was pumped by the Yb-doped fibre laser at a wavelength of 1098 nm separated by 31 nm from the zero-dispersion wavelength (1129 nm) for this fibre. When the signal wavelength λ_{sign} of the Ti : sapphire laser was exactly tuned to the phase-matching wavelength (845 nm), a four-wave mixing signal was observed in a narrow band

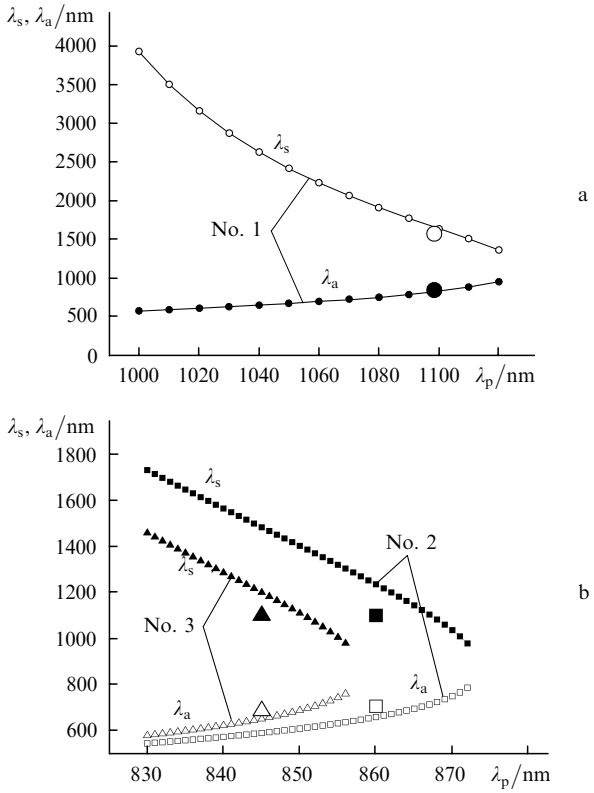

Figure 6. Tuning curves calculated from the phase-matching condition by using experimental dispersion curves for fibres No. 1–3. Large circles, triangles, and squares correspond to experimental shifts (dark points are signal radiation, light points are radiation obtained after four-wave mixing).

(narrower than 0.5 nm) at the wavelength $\lambda_{conv} = 1569$ nm. The conversion efficiency in this fibre of length $L =$ 6 m was $\eta = 5 \times 10^{-4}$ % for a 600-mW pump power. Such a low conversion efficiency is explained not only by a small length of the fibre but also by its low nonlinearity $\gamma = 4$ W^{-1} km^{-1}, which is typical for microstructure silica fibres with the hexagonal structure and dispersion zero in the region above 1 μm.

Two-layer microstructure fibres, which had a much greater blue shift of the dispersion zero, were pumped by the tunable Ti : sapphire laser. Due to four-wave mixing, a signal from the Yb-doped fibre laser at the wavelength $\lambda_{sign} = 1098$ nm was converted in fibre No. 2 to radiation at the wavelength $\lambda_{conv} = 706$ nm upon pumping at $\lambda_p =$ 860 nm and in fibre No. 3 to radiation at $\lambda_{conv} =$ 687 nm upon pumping at $\lambda_p = 845$ nm. The maximum conversion efficiency in fibres No. 2 and 3 was 0.01 % and 0.1 %, respectively. We measured the dependence of the conversion efficiency on the fibre length. The four-wave mixing signal in fibre No. 2 increased with increasing fibre length up to 15 m. The maximum conversion efficiency in fibre No. 3 was obtained for the fibre length $L = 100$ m (Fig. 7). Note also that the width of the tuning band of a

Table 2.

Fibre number	L/m	λ_p/nm	$\lambda_0 - \lambda_p$/nm	λ_{sign}/nm	λ_{conv}/nm	P_0/mW	P_{sign}/mW	P_{conv}/μW	$\eta = \frac{P_{conv}}{P_{sign}}$ (%)
1	6	1098	31	845	1569	600	100	0.5	0.0005
2	15	860	14	1098	706	100	300	30	0.01
3	100	845	13	1098	687	100–200	500–700	550–770	0.11

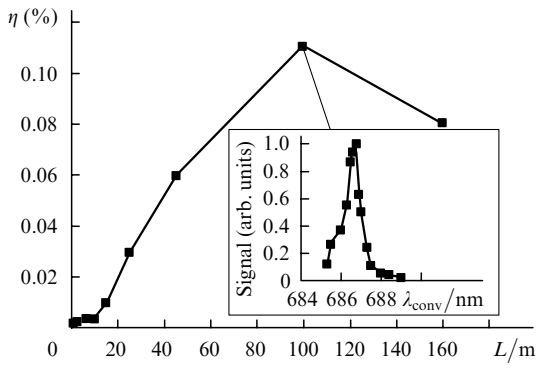

Figure 7. Experimental dependence of the conversion efficiency on the length of two-layer fibre No. 3.The insert shows the band of parametric frequency conversion measured for the maximum conversion efficiency ($L = 100$ m).

signal at $\lambda_{conv} = 687$ nm in fibre No. 3 weakly depended on the fibre length up to $L = 100$ m and was ~ 0.7 nm (FWHM) (insert in Fig. 7). This demonstrates good optical quality of the two-layer microstructure fibre, which provides a stable effective mode area over a large fibre length.

5. Conclusions

We have studied the dispersion, waveguide, and nonlinear properties of two-layer microstructure fibres with different layer filling factors. It has been shown theoretically that by increasing the filling factor of the second layer compared to the first layer, we can obtain a smaller effective mode area, expand the wavelength range in which the mode localisation is possible, and achieve a better control of dispersion characteristics than in the case of identical filling factors. A signal radiation wavelength of 1098 nm has been converted to radiation at 687 nm with the efficiency 0.1 % due to four-wave mixing upon 200-mW cw pumping two-layer fibres of length ~ 100 m with the filling factor $\kappa_2 > \kappa_1$.

Acknowledgements. The authors thank Dr. Sebastian Fevrier of the IRCOM Institute, the University of Limoges (France) for his help in numerical calculations.

References

1. Agraval G. *Nonlinear Fibre Optics* (San Diego: Academic Press, 1995; Moscow: Mir, 1996).
2. Mashinsky V.M., Neustruev V.B., Dvoyrin V.V., Vasiliev S.A., Medvedkov O.I., Bufetov I.A., Shubin A.V., Dianov E.M., Guryanov A.N., Khopin V.F., Salgansky M.Yu. *Opt. Lett.*, **15**, 2596 (2004).
3. Tanaka K., Narasaki A., Hirao K. *Opt. Lett.*, **25**, 251 (2000).
4. Lee J.H., Nagashima T., Hasegava T., Ohara S., Sugimoto N., Tanemura T., Kikuchi K. *Proc. OFC 2005* (Anaheim, CA, USA, 2005) PDP23.
5. Stolen R.H., Bjorkholm J.E., Ashkin A. *Appl. Phys. Lett.*, **24**, 308 (1974).
6. Stolen H., Bosh M.A., Lin C. *Opt. Lett.*, **6**, 213 (1981).
7. Knight J.S., Birks T.A., Russel P.St.J., Atkin D.M. *Opt. Lett.*, **21**, 547 (1996).
8. Knight J.C., Birks T.A., Russel P.St. J., de Sandro J.P. *J. Opt. Soc. Am. A*, **15**, 748 (1998).
9. Knight J.C., Arriaga J., Birks T.A. *IEEE Photonic Technol. Lett.*, **12**, 807 (2000).
10. Wadsworth W.J., Joly N., Knight J.C., Birks T.A., Biancalana F., Russell P.St. J. *Opt. Express*, **12**, 299 (2004).
11. Andersen T.V., Hilligsoe K.M., Nielsen C.K., Thogersen J., Hansen K.P., Keiding S.R., Larsen J.J. *Opt. Express*, **12**, 4113 (2004).
12. Ferrando A., Silvestre E., Andres P., Mirret J.J., Andres M.V. *Opt. Express*, **13**, 687 (2001).
13. Monro T.M., Richardson D.J., Broderick N.G., Bennett P.J. *J. Lightwave Technol.*, **17**, 1093 (1999).
14. Koshiba M., Saitoh K. *Opt. Express*, **11**, 1746 (2003).
15. Ferrarini D.,Vincetti L., Zoboli M. *Proc. OFC 2003* (Atlanta, GA, USA, 2003) Vol. 2, F15, 23.
16. Belov A.V., Dianov E.M. *Kvantovaya Elektron.*, **32**, 641 (2002) [*Quantum Electron.*, **32**, 641 (2002)].
17. Saitoh K, Koshiba M., Hasegava T., Sasaoka E. *Opt. Express*, **11**, 843 (2003).
18. Poletti F., Finazzi V., Monro T.M., Broderick N.G.R., Tse V., Richardson D.J. *Opt. Express*, **13**, 3728 (2005).
19. Belov A.V., Dianov E.M., Kurkov A.S. *Kvantovaya Elektron.*, **13**, 1680 (1986) [*Sov. J. Quantum Electron.*, **16**, 1096 (1986)].
20. Levchenko A.E., Kurkov A.S., Semenov S.L. *Kvantovaya Elektron.*, **35**, 835 (2005) [*Quantum Electron.*, **35**, 835 (2005)].